# Structure of Adsorbed Polyampholyte Layers at Charged Objects

**Andrey V. Dobrynin, Ekaterina B. Zhulina, and Michael Rubinstein***

*Department of Chemistry, University of North Carolina, Chapel Hill, North Carolina 27599-3290*

*Received April 21, 2000; Revised Manuscript Received September 22, 2000*

ABSTRACT: We have developed a theory of adsorption of polyampholyte chains at a charged planar surface and a charged spherical particle from dilute low salt solutions. The adsorption is due to the polarization of polyampholyte chains in the external electric field created by charged objects. The equilibrium polymer density profile is determined by the balance of the long-range polarization-induced attraction of polyampholytes to the charged object and the monomer−monomer repulsion. We demonstrate that the long-range nature of polyampholyte adsorption leads to an adsorbed layer much thicker than the size of individual chains. Using the self-consistent mean-field and scaling approaches, we obtain the detailed structure of the adsorbed layers.

## I. Introduction

The adsorption of polymers at surfaces and interfaces has been under extensive theoretical and experimental studies during the last four decades.[1−3] This interest was stimulated by the tremendous importance of this problem for different areas of natural sciences ranging from materials science to biophysics. The advancements in understanding of this complicated problem have found their applications in bioengineering, colloid stabilization, wetting, adhesion, lubrication, etc.

The attraction between polymer and surfaces can be caused by short-range van der Waals interactions and long-range electrostatic interactions. In the case of short-range interactions the adsorbing polymer chains build up a fluffy layer in the vicinity of the attractive surface where they form a self-similar de Gennes' carpet[2,4] of loops and tails with broad distribution in sizes. If polymer adsorbs from a dilute solution, the thickness of the adsorbed layer is on the order of the size of an isolated chain.

In the case of the Coulomb interaction the experimental[1−3,5,6] and theoretical[2,7−19] studies were mainly limited to the adsorption of polyelectrolytes—polymers carrying either positively or negatively charged groups. Polyampholytes, which are amphoteric polymers with both positively and negatively charged groups, have received less theoretical[20−22] and experimental[23−30] attention. The theoretical studies of polyampholyte adsorption[20−22] revealed a new mechanism that is due to polarization of chains in the external electric field created by charged objects. Because of the long-range nature of the polarization-induced attractive interactions between polyampholyte chains and charged objects, macromolecules build up multiple polymeric layers near adsorbing surfaces. The adsorption stops at the distances from the adsorbing surface where the external electric field created by the charged surface is not strong enough to polarize the polyampholyte chain. The thickness of the polymer coating depends on charge distribution along the polymer backbone, which determines polarizability of polyampholyte chains in external electric fields.[31−35] At equilibrium the long-range polarization-induced attraction is balanced by the short-range monomer−monomer repulsion.[22]

In the present paper, we address the structure of the adsorbed layer formed by weakly charged polyampholyte chains near charged planar and spherical surfaces and calculate the polymer density profile as well as the distributions of loops and tails for both geometries.

## II. Adsorption at a Charged Planar Surface[22]

Consider the adsorption of symmetric weakly charged polyampholyte chains with equal fraction of positively $f_+ = f/2$ and negatively $f_- = f/2$ charged monomers from a dilute solution with dielectric constant $\epsilon$ onto an infinite plane with $\sigma$ elementary charges per unit area. In the absence of added salt, the electric field created by this plane decays with distance $z$ from the surface[36] as

$$E(z) = \frac{4\pi e\sigma}{\epsilon(1 + z/\lambda)} \tag{1}$$

where $e$ is the elementary charge, $\lambda = (2\pi l_B\sigma)^{-1}$ is the Gouy−Chapman length inside which the significant fraction of counterions is localized, and $l_B = e^2/\epsilon kT$ is the Bjerrum length at which two elementary charges interact with energy $kT$. The size $L(z)$ of a polyampholyte chain containing $N$ monomers, connected by bonds of length $a$, immersed in a Θ solvent at distance $z$ from the charged surface can be estimated by balancing the electrostatic energy of the dipole of two opposite charges $\pm eq$ of the two halves of the chain separated by the distance $L(z)$ in the external electric field $E(z)$ with the elastic stretching energy[20,21]

$$E(z)eqL(z) \approx kT\frac{L(z)^2}{a^2N} \tag{2}$$

If the positions of the charges along the chain are uncorrelated, this chain has, on average, $|q| \approx \sqrt{fN}$ excess of positive or negative charges on the halves of the chain. For this type of polyampholytes the balance leads to the size of the chain perpendicular to the surface

$$L(z) \approx \frac{E(z)ef^{1/2}N^{3/2}a^2}{kT} \approx \frac{R_0{}^2\sqrt{fN}}{(\lambda + z)} \tag{3}$$

where $R_0 \approx a\sqrt{N}$ is the Gaussian size of a chain. At

10.1021/ma000706d CCC: $20.00 
Published on Web 12/21/2000

distances $z$ from the surface shorter than the Gouy−Chapman length $\lambda$, the size of the chain perpendicular to the surface grows linearly with the surface charge density $\sigma$

$$L \approx \frac{R_0^2\sqrt{fN}}{\lambda} \approx R_0^2 l_B \sigma \sqrt{fN}, \quad \text{for } z < \lambda \tag{4}$$

The deformation of the chain from its Gaussian shape begins at the surface charge density $\sigma$ larger than the marginal surface charge density

$$\sigma_1 \approx \frac{1}{a l_B f^{1/2} N^{3/2}} \approx \frac{1}{l_B R_0 (fN)^{1/2}} \tag{5}$$

At lower surface charge densities $\sigma < \sigma_1$, the electric field created by charged surface is too weak to polarize the chain and polyampholyte does not adsorb. The polarization energy of the polyampholyte chain in the external electric field $E(z)$ given by eq 1 is

$$W_{pol}^{ch}(z) \approx -kT\left(\frac{\lambda_1}{z+\lambda}\right)^2 \tag{6}$$

where we have introduced the threshold Gouy−Chapman length

$$\lambda_1 \approx 1/(l_B\sigma_1) \approx R_0\sqrt{fN} \tag{7}$$

At surface charge densities $\sigma$ above the adsorption threshold value $\sigma_1$, this polarization leads to attraction and adsorption of polyampholytes at the surface that is stabilized by the repulsion between monomers. In a $\Theta$ solvent for the polymer backbone this repulsive interaction is due to three-body contacts. The three-body repulsion energy per monomer can be approximated by

$$W_{rep}(z) \approx kTa^6c^2(z) \tag{8}$$

where $c(z)$ is the concentration of monomers at distance $z$ from the charged surface. The total free energy of polyampholyte chains per unit area in the adsorbed layer is

$$F \approx kT\int\left(-\frac{c(z)}{N}\left(\frac{\lambda_1}{z+\lambda}\right)^2 + a^6c^3(z)\right)dz \tag{9}$$

The minimization of the free energy (9) with respect to the monomer concentration $c(z)$ results in the equilibrium density profile

$$c(z) \approx c_0^*\frac{\lambda_1}{z+\lambda} \tag{10}$$

where $c_0^* \approx a^{-3}N^{-1/2}$ is the overlap concentration. At distances $z$ larger than the Gouy−Chapman length $\lambda$, we expect the hyperbolic density profile $c(z) \approx c_0^*\lambda_1/z$. Near the charged surface, the polymer density saturates at $c(0) \approx c_0^*\lambda_1/\lambda$. The crossover between the semidilute and dilute regime of the adsorbed chains occurs at the distance $z \approx \lambda_1$. At this distance $z \approx \lambda_1$ the attractive interaction between polyampholytes and the charged surface becomes comparable with the thermal energy $kT$ per chain. Therefore, one can consider $\lambda_1$ as the thickness of the adsorbed layer. The excess adsorbed amount $\Gamma$ per unit surface area is

$$\Gamma \approx \int_0^{\lambda_1} c(z)\,dz \approx a^{-2}\sqrt{fN}\ln\left(\frac{\sigma}{\sigma_1}\right) \tag{11}$$

The polymer excess can be significantly higher than that for the adsorption at an uncharged surface[2] $\Gamma \approx a^{-2}$ and grows logarithmically with the surface charge density.

As the surface charge density $\sigma$ increases, the Gouy−Chapman length $\lambda$ decreases and becomes comparable with the size of the chain $L \approx l_B\sigma R_0^2\sqrt{fN}$ near the surface at the surface charge density $\sigma$ on the order of

$$\sigma_2 \approx \frac{1}{a l_B f^{1/4} N^{3/4}} = \frac{1}{l_B R_0 (fN)^{1/4}} \tag{12}$$

At higher surface charge densities ($\sigma > \sigma_2$), the size of the chains in the first adsorbed layer saturates at $L \approx \lambda_2$ where

$$\lambda_2 \approx 1/l_B\sigma_2 \tag{13}$$

The adsorbed layer at the length scales $z < \lambda_2$ can be viewed as a self-similar pseudobrush of stretched polydisperse loops (see Figure 1). The detailed calculations of the structure of this self-similar layer in the framework of the self-consistent mean-field approach are presented in the Appendix. Below we use simple scaling arguments[22] that produce similar results.

The stretching of a subsection containing $g(z)$ monomers with size $z_g$ can be estimated by balancing the elastic energy of this subsection $kTz^2/(a^2g(z))$ by its polarization energy $e\sqrt{fg(z)}zE(z)$. At the length scales $z > \lambda$ the electric field $E(z) \approx e/(\epsilon l_B z)$ is inversely proportional to the distance $z$ from the surface. The relation between the strand size $z$ and the number of monomers $g(z)$ in it is given by the following equation:

$$z_g \approx a\sqrt{g}(fg)^{1/4}, \quad \text{for } \lambda < z_g < \lambda_2 \tag{14}$$

The polarization energy per strand of $g$ monomers is proportional to $-kT\sqrt{fg(z)}$. The density of polarization energy $U_{pol}(z)$ of polyampholytes at distance $z$ from the surface is equal to the concentration of the strands $c(z)/g(z)$ containing $g(z)$ monomers times the polarization energy per strand

$$\frac{U_{pol}(z)}{kT} \approx -c(z)\left(\frac{af}{\lambda+z}\right)^{2/3} \tag{15}$$

The balance of this polarization energy density and the three-body repulsion $a^6c^3(z)$ leads to the equilibrium density profile (see Appendix for details)

$$c(z) \approx a^{-3}\left(\frac{af}{\lambda+z}\right)^{1/3} \tag{16}$$

Closer to the surface (for $z < \lambda$) the density $c(z)$ is almost uniform and saturates at $a^{-3}(af/\lambda)^{1/3}$. At length scales $z$ larger than the Gouy−Chapman length, the monomer density decays as $z^{-1/3}$. For this density profile the loop distribution function − number of loops or tails (with $2g$ monomers) per unit area is

$$\rho_g \approx \begin{cases} a^{-2}f^{1/2}g^{-3/2}, & \text{for } g_\lambda < g < N \\ 0, & \text{for } g < g_\lambda \end{cases} \tag{17}$$

where $g_\lambda = \lambda^{4/3}a^{-4/3}f^{-1/3}$ is the number of monomers in a loop with size on the order of the Gouy−Chapman

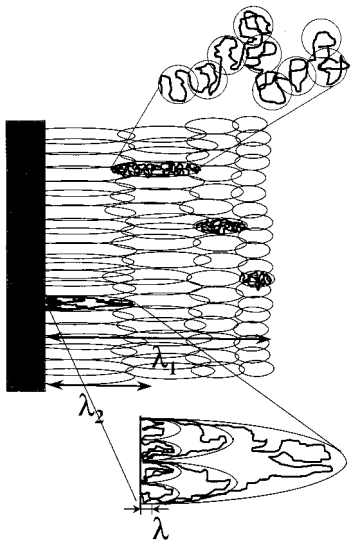


**Figure 1.** Schematic sketch of the configurations of polyampholyte chains near a charged planar surface.

length $\lambda$. This distribution function eq 17 was derived in the Appendix and tells us that there are no loops with sizes smaller than the Gouy−Chapman length (see Figure 1). This is due to the fact that a loop with $g_\lambda$ monomers will have the lowest free energy in the constant electric field $E \approx e/(\epsilon l_B \lambda)$ inside the Gouy−Chapman length $\lambda$. In fact, the probability to find a smaller loop is exponentially low.

At length scales larger than $\lambda_2$ the density has the same hyperbolic profile as described above in eq 10. The thickness of the adsorbed layer is still $\lambda_1$ and the polymer excess in this regime is

$$\Gamma \approx \int_0^{\lambda_1} c(z)\,dz \approx \int_{\lambda_2}^{\lambda_1} c(z)\,dz \approx a^{-2}\sqrt{fN}\,\ln(fN) \qquad (18)$$

In the case of a very high surface charge density ($\sigma > \sigma_3 \approx f^{1/2}/(al_B)$), the Gouy−Chapman length $\lambda$ is smaller than the root-mean-square distance between charged monomers $af^{-1/2}$. The size of polyampholyte molecules in the first adsorbed layer is still $\lambda_2$, but these chains are self-similarly stretched on all length scales between the smaller distance

$$\lambda_3 \approx af^{-1/2} \qquad (19)$$

and $\lambda_2$. In the layer of thickness $\lambda_3$ near the wall the monomer density is constant and is proportional to $c \approx a^{-3}f^{1/2}$. At the distance scales between $\lambda_2$ and $\lambda_1$ one finds multibrush of stretched chains. The excess adsorbed amount $\Gamma$ for the range of surface charge densities $\sigma > \sigma_3$ is still given by eq 18.

## III. Adsorption at a Charged Spherical Particle

Consider the adsorption of polyampholytes at a charged spherical particle with radius $R$ and surface charge density $e\sigma = eQ/4\pi R^2$, where $eQ$ is the total charge on the particle. The equal number of the monovalent counterions, $Q$, is distributed in solution around the particle. At small distances $r - R \ll R$ from the surface of the sphere, its curvature is not important, and the electrostatic potential can be approximated by that for a planar surface with the charge density $e\sigma$

$$\varphi(r) \approx \frac{eQ}{\epsilon R} - 2\frac{kT}{e}\ln\left(1 + \frac{r-R}{\lambda}\right), \quad \text{for } r - R \ll R \qquad (20)$$

The structure of the adsorbed layer will be unaffected by the curvature of the particle as long as the particle size $R$ is larger that the thickness of the adsorbed layer $\lambda_1$ in the planar case. Thus, the condition

$$R \approx \lambda_1 \approx R_0\sqrt{fN} \qquad (21)$$

is the lower boundary for the planar regime. For the smaller charged particles, $R < \lambda_1$, there will be a new structure of the adsorbed layer at the distances $r - R \geq R$ while inside the layer of the thickness $r - R \leq R$ the layer structure is similar to the one discussed in the previous section.

The counterions distributed near the surface of the particle at distances $r - R \leq R$ inside the layer of the thickness $R$ screen the charge on the particle. The effective charge $Q_{eff}$ at distance $2R$ from the center of the sphere can be estimated by integrating the counterion density profile near the surface of the particle

$$n(r) \approx \frac{1}{2\pi l_B(\lambda + r - R)^2}, \quad \text{for } r - R \ll R \qquad (22)$$

between $R$ and $2R$

$$Q_{eff} \approx Q - 4\pi R^2 \int_R^{2R} n(r)\,dr \approx \frac{Q\lambda}{(\lambda + R)} \qquad (23)$$

If the Gouy−Chapman length $\lambda$ is much smaller than the size of the particle, $R$, the counterions are localized inside the planar region $r - R \ll R$ and electrostatic potential is significantly screened. The effective charge on the sphere, that the rest of the solution beyond the pseudo-planar layer ($r - R \leq R$) "feels", saturates at

$$Q_{eff} \approx R/l_B \qquad (24)$$

and does not depend on the bare charge $Q$ of the particle.[37] At distances $r - R \gg R$, the electrostatic potential is that of the charged sphere with the effective charge $Q_{eff}$

$$\varphi(r) \approx \frac{eQ_{eff}}{\epsilon r} + C \qquad (25)$$

while at distances $r - R \ll R$, the potential is described by eq 20. The constant

$$C \approx \frac{eQ}{\epsilon R} - 2\frac{kT}{e}\ln\left(1 + \frac{R}{\lambda}\right)$$

is determined by the continuity of the potential at $r \approx 2R$.

However, if the size of the particle $R$ is smaller than the Gouy−Chapman length $\lambda$ the screening of the electrostatic potential by the counterions can be neglected ($Q_{eff} \approx Q$). In this case the potential is inversely proportional to the distance $r$ from the center of the sphere

$$\varphi(r) \approx \frac{eQ}{\epsilon r} \qquad (26)$$

**A. Strongly Charged Particles $\lambda < R$.** In the case of strongly charged particles when the charge on the

sphere is significantly screened by the counterions, the polarization energy of a polyampholyte chain of size $L(r)$ with the center of mass located at the distance $r \gg R$ from the center of the particle is

$$\frac{W_{\text{pol}}^{\text{ch}}(r)}{kT} \approx l_B Q_{\text{eff}} \sqrt{fN}\left(\frac{1}{r + L(r)} - \frac{1}{r - L(r)}\right) \approx -\frac{R\sqrt{fN}}{r^2 - L(r)^2} L(r) \quad (27)$$

Balancing the polarization energy of the chain with its elastic energy $kTL(r)^2/(a^2N)$ we can obtain the chain size as a function of the distance from the particle. At length scales $r \gg L(r)$ the chain size is

$$L(r) \approx \frac{a^2 l_B Q_{\text{eff}} f^{1/2} N^{3/2}}{r^2} \approx R_0^2 \frac{R\sqrt{fN}}{r^2} \quad (28)$$

The deformation of the chain from its Gaussian conformation ($L(r) > R_0$) begins at distances $r$ on the order of

$$r_1 \approx (R_0 R\sqrt{fN})^{1/2} \approx \sqrt{R\lambda_1} \approx (a l_B Q_{\text{eff}} f^{1/2} N)^{1/2} \quad (29)$$

This distance $r_1$ decreases with decreasing particle size $R$. The polarization energy of a polyampholyte chain near the charged spherical particle for the distances $r - R \gg R$ is

$$\frac{W_{\text{pol}}^{\text{ch}}(r)}{kT} \approx -\left(\frac{r_1}{r}\right)^4, \quad \text{for } r - R \gg R \quad (30)$$

This polarization energy of the chain has stronger distance dependence than the one obtained for the case of a charged planar surface (see eq 6). The equilibrium density profile $c(r)$ around a charged spherical particle corresponds to the minimum of the following density functional

$$\frac{F}{kT} \approx \int_{2R}^{r_1}\left(-\frac{c(r)}{N}\left(\frac{r_1}{r}\right)^4 + a^6 c^3(r)\right) r^2 \, dr \quad (31)$$

and is equal to

$$c(r) \approx c_0^* \left(\frac{r_1}{r}\right)^2 \approx c_0^* \frac{R\lambda_1}{r^2}, \quad \text{for } 2R < r < r_1 \quad (32)$$

At distances $r < r_1$ the adsorbed polyampholyte chains are strongly stretched and overlap with each other. The crossover to the dilute regime occurs at distances r on the order of the marginal distance $r_1 \approx \sqrt{R\lambda_1}$. In the case of the spherical particle, the adsorbed layer is thinner than that in the case of the planar surface because $\sqrt{R\lambda_1} < \lambda_1$ for a particle size $R$ smaller than the marginal Gouy−Chapman length $\lambda_1$. Closer to the surface of the particle at length scales $r - R < R$, the curvature of the particle is irrelevant and the structure of the adsorbed layer is the same as in the planar case described in the section II. The polymer density profile near the charged spherical particle is shown in Figure 2.

Integrating the polymer density profile between $R < r < r_1$, we obtain the dependence of the surface coverage

$$\Gamma \approx \frac{1}{R^2}\int_R^{r_1} c(r) r^2 \, dr \quad (33)$$

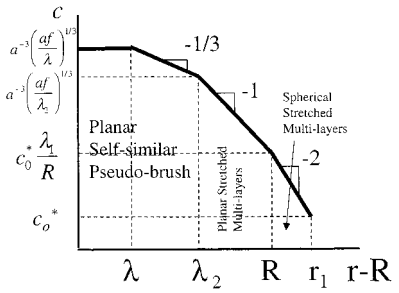


**Figure 2.** Polymer density profile in the adsorbed layers in a Θ solvent for $\lambda_2 < R < \lambda_1$. Logarithmic scales.

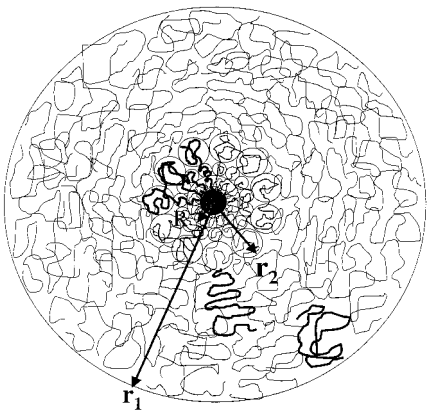


**Figure 3.** Schematic sketch of the structure of the adsorbed polyampholyte chains at a charged spherical particle.

on the particle size, that scales as

$$\Gamma \approx a^{-2}\sqrt{fN\frac{\lambda_1}{R}} + \begin{cases} a^{-2}\sqrt{fN}\ln\left(\frac{R}{\lambda}\right), & \text{for } \sigma_1 < \sigma < \sigma_2 \text{ and } \lambda_2 < R < \lambda_1 \\ a^{-2}\sqrt{fN}\ln\left(\frac{R}{\lambda_2}\right), & \text{for } \sigma_2 < \sigma \text{ and } \lambda_2 < R < \lambda_1 \end{cases} \quad (34)$$

The first term in the last equation is due to the outer part of the adsorbed layer, $2R < r < r_1$, and controls the overall adsorbed amount for particles with size $R \ll \lambda_1$.

For adsorption of polyampholyte chains at a charged planar surface with the surface charge densities $\sigma$ larger than the marginal surface charge density $\sigma_2$ the size of the chains in the first adsorbed layer saturates at $\lambda_2$. Inside the layer of thickness $\lambda_2$ the chains form a self-similar polydisperse brush of loops (see section II for details). This self-similar structure begins to be affected by the curvature of the particle at the particle size $R$ on the order of the layer thickness $\lambda_2$. For smaller particles ($R < \lambda_2$) there are two different types of loops. Close to the surface of the charged particle, inside the layer of thickness $r - R \lesssim R$, the loop structure and loop distribution function $\rho_g$ are similar to the one in the planar case (see section II and Figure 3). In the outer region, at distances $r$ from the center of the particle larger than $2R$, we have a different self-similar structure formed by the loops with distribution function determined by their polarization in the hyperbolic electrostatic potential (see Appendix for details). Below, we again use simple scaling arguments to determine the structure of the adsorbed layer at distances $r \gg 2R$.

The polarization energy of a loop containing $g$ monomers with the center of mass located at distance $r - R \gg R$ from surface of the particle with the excess charges in two halves of a loop $q \approx (fg)^{1/2}$ separated by the distance $r$, is given by the following expression:

$$\frac{W_{pol}}{kT} \approx -\frac{qR}{r} \approx -\frac{\sqrt{fg(r)}R}{r} \tag{35}$$

The relation between the loop size $r$ and the number of monomers $g$ in it is obtained by the balance of the loop polarization energy $W_{pol}$, eq 35, with its elastic energy, $F_{el} \approx kTr^2/ga^2$, to give

$$g(r) \approx \frac{r^2}{a^{4/3}f^{1/3}R^{2/3}}, \quad \text{for } r - R > R \tag{36}$$

The density of polarization energy $U_{pol}(r)$ at distance $r$ from the center of sphere is equal to the concentration of the loops $c(r)/g(r)$ with $g(r)$ monomers times the polarization energy of a loop $W_{pol}(r) \approx -\sqrt{fg(r)}R/r$

$$\frac{U_{pol}(r)}{kT} \approx -c(r)\sqrt{\frac{f}{g(r)}}\frac{R}{r} \approx -c(r)f^{2/3}\frac{R^{4/3}a^{2/3}}{r^2}, \quad \text{for } r > 2R \tag{37}$$

The balance of this polarization energy density and the three-body repulsion $a^6c(r)^3$ leads to the equilibrium density profile

$$c(r) \approx a^{-3}\frac{a^{1/3}f^{1/3}R^{2/3}}{r}, \quad \text{for } r > 2R \tag{38}$$

The polymer density profile in this self-similar layer is inversely proportional to the distance from the charged spherical particle and decreases faster than that for a charged planar surface ($c(z) \approx z^{-1/3}$). The radius of this layer $r_2$ can be obtained by substituting $g \approx N$ into rhs of eq 36. This results in

$$r_2 \approx a^{2/3}(l_B f^{1/2}Q_{eff})^{1/3}N^{1/2} \approx (\lambda_2^2 R)^{1/3} \approx a^{2/3}R^{1/3}f^{1/6}N^{1/2} \tag{39}$$

For this particular structure of the adsorbed layer the loop distribution function is a $\delta$ function (see Appendix for details)

$$\rho(g) \approx \frac{1}{R^2}\left(\frac{l_B{}^2Q_{eff}{}^2f}{a^2}\right)^{2/3}\delta(g - N), \quad \text{for } g_{2R} < g < N \tag{40}$$

where $g_{2R}$ is the number of monomers in the loop of size $2R$. Thus, the structure of the adsorbed layer at length scales $R < r - R < r_2$ is similar to the one for a star polymer in a $\Theta$ solvent[38,39] with all end points of loops located at the periphery of the outer layer of the thickness $r_2$. The number of chains in the layer of the thickness $r_2$ (branches of a star) can be estimated by integrating the polymer density profile

$$n_{ch} \approx N^{-1}\int_{2R}^{r_2} c(r)r^2\,dr \approx \left(\frac{l_B{}^2Q_{eff}{}^2f}{a^2}\right)^{2/3} \approx \left(\frac{R^2f}{a^2}\right)^{2/3} \tag{41}$$

The number of chains forming this layer decreases with decreasing particle size. The schematic sketch of the chains in the adsorbed layer is shown in Figure 3. Adsorbed polyampholyte chains form a pseudo-brush of loops inside the layer of the thickness $R$ from the particle surface. The structure of this pseudo-brush inside the layer with thickness $R$ is similar to the one in the case of adsorption at a planar surface (see Figure 1). The outer layer ($R \ll r - R \ll r_2$) is formed by large loops that can be envisioned as branches attached to the core of a pseudo-star molecule with radius $R$. These branches overlap with each other with distance-dependent correlation length $\xi(r) \sim n_{ch}{}^{-1/2}r$. The polymer density profile $c(r) \approx \xi^{-1} \approx n_{ch}{}^{1/2}r^{-1}$ inside this layer agrees with the scaling model of starlike polymer in a $\Theta$ solvent.[38,39]

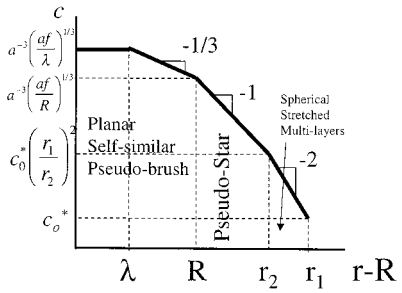


**Figure 4.** Polymer density profile in the adsorbed layers in a $\Theta$ solvent for $\lambda < R < \lambda_2$. Logarithmic scales.

At length scales $r_2 < r < r_1$, the polymer density profile in spherical stretched multilayers is still given by eq 32. The polymer density profile in this regime is shown in Figure 4.

The polyampholyte chains desorb from the particle when the polarization energy of the chains in the first layer of the thickness $r_2$

$$W_{pol} \approx -kTa^6\int_R^{r_2} c^3(r)r^2\,dr \approx -kT\,f\frac{R^2}{a^2}\ln\left(\frac{r_2}{R}\right) \tag{42}$$

becomes on the order of the thermal energy $kT$. This occurs when the particle size $R$ becomes on the order of the typical distance $af^{-1/2}$ between charged monomers.

**B. Weakly Charged Particles $\lambda > R$.** In the case of weakly charged particles the electrostatic interaction between polyampholytes and the charged sphere is unscreened. Repeating the same calculations as in the previous section we can rewrite the polarization energy of a polyampholyte chain, eq 27, for the case of unscreened Coulomb potential

$$\frac{W_{pol}^{ch}(r)}{kT} \approx -\frac{l_BQ\sqrt{fN}}{r^2 - L(r)^2}L(r) \tag{43}$$

Once again the balance of the polarization energy of the chain and its elastic energy gives the chain size at the distance $r$ from the particle. (See eq 28.)

$$L(r) \approx \frac{a^2l_BQf^{1/2}N^{3/2}}{r^2} \approx \frac{l_BQR_0{}^2\sqrt{fN}}{r^2} \approx \frac{l_BQ\lambda_1}{r^2} \tag{44}$$

Substituting this equilibrium chain size $L(r)$ back into expression 43, we obtain the polarization energy of a polyampholyte chain

$$\frac{W_{pol}^{ch}(r)}{kT} \approx -\frac{(l_BQ\lambda_1)^2}{r^4} \approx -\left(\frac{r_1}{r}\right)^4 \tag{45}$$

where

$$r_1 \approx \sqrt{l_B Q \lambda_1} \approx \sqrt{l_B Q R_0 \sqrt{fN}} \quad (46)$$

is the distance at which the polarization energy becomes on the order of the thermal energy $kT$. The balance between the polarization-induced attraction eq 45 and the three-body repulsion eq 8 results in the equilibrium polymer density profile

$$c(r) \approx c_0^* \left(\frac{r_1}{r}\right)^2 \approx c_0^* \frac{l_B Q R_0 \sqrt{fN}}{r^2}, \quad \text{for } r < r_1 \quad (47)$$

At length scales $r < r_1$ the adsorbed polyampholytes form a spherical multilayer of stretched chains. The excess adsorbed amount $\Gamma$ per unit surface area of the charged particle is

$$\Gamma \approx \frac{1}{R^2} \int_R^{r_1} c(r) r^2 dr \approx c_0^* \frac{r_1^3}{R^2} \quad (48)$$

The surface excess increases with decreasing particle size.

The stretching of a polyampholyte chain as a whole in the adsorbed layer continues until its size $L(r)$ becomes on the order of its distance to the particle surface $r$

$$r_2 \approx (a^2 l_B Q f^{1/2} N^{3/2})^{1/3} \approx (R_0 r_1^2)^{1/3} \quad (49)$$

At length scales $r_2 < r < r_1$, adsorbed polyampholytes form a spherical multilayer of stretched chains while at length scales $r < r_2$ the adsorbed polyampholytes form a pseudo-star. The structure of the polydisperse brush of loops in a pseudo-star is similar to the one discussed in the previous section, where in all equations the effective charge $Q_{eff}$ has to be substituted by the bare charge $Q$.

In this case, at length scales $R < r - R < r_2$, the relation between the strand size $r$ and the number of monomers $g(r)$ in it is

$$r \approx a^{1/3} (l_B f^{1/2} Q)^{1/3} g(r)^{1/2}, \quad \text{for } R < r - R < r_2 \quad (50)$$

The polymer density in this self-similar layer is inversely proportional to the distance $r$ from the center of a particle.

$$c(r) a^3 \approx \frac{a^{1/3} (l_B Q)^{2/3} f^{1/3}}{r} \approx c_0^* a^3 \frac{r_1^{4/3}}{R_0^{1/3} r}, \quad \text{for } R < r - R < r_2 \quad (51)$$

The number of chains in the layer of the thickness $r_2$ is on the order of

$$n_{ch} \approx N^{-1} \int_R^{r_2} c(r) r^2 dr \approx \left(\frac{l_B f^{1/2} Q}{a}\right)^{4/3} \quad (52)$$

and depends only on the charge of the particle $Q$ and on the fraction of the charged monomers $f$ on polyampholyte chains.

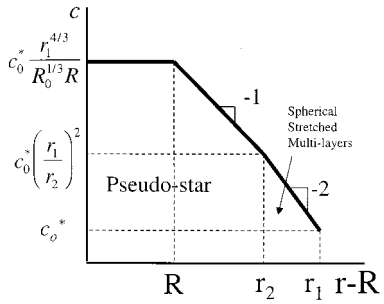


**Figure 5.** Polymer density profile in the adsorbed layers in a $\Theta$ solvent for $R < \lambda$. Logarithmic scales.

Integrating the polymer density profile between $R$ and $r_1$ one obtains the polymer adsorbed amount

$$\Gamma \approx \frac{N}{R^2} (n_{ch} + n_{ch}^{9/8}) \approx \frac{N}{R^2} \left(\frac{l_B f^{1/2} Q}{a}\right)^{3/2} \quad (53)$$

which is dominated by the outer region $r_2 < r < r_1$. The surface coverage increases with increasing charge $Q$ of the particle.

As the charge $Q$ of the particle decreases, the thickness $r_1$ of the multilayer decreases as well. This layer disappears completely when the layer thickness $r_1$ becomes on the order of the thickness $r_2$ of the pseudo-star. This occurs when the charge $Q$ of the particle is

$$Q \approx \frac{a}{l_B} f^{-1/2} \quad (54)$$

At this value of the charge $Q$, there will be only one adsorbed polyampholyte chain with the polarization energy

$$W_{pol} \approx -kT a^6 \int_R^{r_2} c^3(r) r^2 \, dr \approx -kTf \left(\frac{l_B Q}{a}\right)^2 \ln\left(\frac{r_2}{R}\right) \approx kT \quad (55)$$

on the order of the thermal energy $kT$. Therefore, eq 54 determines the adsorption−desorption threshold for weakly charged particles.

## IV. Conclusion

By using scaling arguments and self-consistent-field calculations, we have described adsorption of polyampholytes at a charged planar surface and a charged spherical particle. The polymer equilibrium density profile in the adsorbed layer is determined by the balance of polarization-induced attraction of the chains to the charged surface and short-range repulsion between monomers. Because of the long-range nature of polarization-induced attraction the adsorbed layer is much thicker than the size of individual chains. We focus on the saturated adsorbed layers which are formed at relatively higher concentration of polymers in solutions $c \approx c_0^*$. The adsorption isotherm for polyampholyte adsorption at charged objects will be discussed in a separate publication.

The results of the paper are summarized in Table 1 and in Figure 6 which represents the effect of the particle size $R$ on the structure of the saturated adsorbed layer. The $x$ axis of the diagram of states (Figure 6) is the parameter $\lambda$, which is equal to the Gouy−Chapman length $\lambda \approx (l_B \sigma)^{-1}$ for the planar surface and to $\lambda \approx R^2/l_B Q$ for the spherical particle with size $R$ and

**Table 1. Thickness of the Adsorbed Layer *H*, Surface Coverage Γ, and Polymer Density Profile in Different Regimes of the Adsorption Diagram (Figure 6)**

| | *H* | Γ | *c* |
|---|---|---|---|
| I | $\lambda_1$ | $a^{-2}\sqrt{fN}\ln\left(\frac{\lambda_1}{\lambda}\right)$ | $c_0^*\frac{\lambda_1}{r-R+\lambda}$ |
| II | $\lambda_1$ | $a^{-2}\sqrt{fN}\ln fN$ | $c_0^*\frac{\lambda_1}{r-R+\lambda}$, for $\lambda_2 < r-R < \lambda_1$<br>$a^{-3}\left(\frac{af}{r-R+\lambda}\right)^{1/3}$, for $0 < r-R < \lambda_2$ |
| III | $\lambda_1$ | $a^{-2}\sqrt{fN}\ln fN$ | $c_0^*\frac{\lambda_1}{r-R+\lambda}$, for $\lambda_2 < r-R < \lambda_1$<br>$a^{-3}\left(\frac{af}{r-R+\lambda_3}\right)^{1/3}$, for $0 < r-R < \lambda_2$ |
| Ia | $\sqrt{R\lambda_1}$ | $a^{-2}\sqrt{fN}\left(\sqrt{\frac{\lambda_1}{R}}-1+\ln\left(\frac{R}{\lambda}\right)\right)$ | $c_0^*\frac{R\lambda_1}{r^2}$, for $2R < r < \sqrt{R\lambda_1}$<br>$c_0^*\frac{\lambda_1}{r-R+\lambda}$, for $0 < r-R < R$ |
| IIa | $\sqrt{R\lambda_1}$ | $a^{-2}\sqrt{fN}\left(\sqrt{\frac{\lambda_1}{R}}-1+\ln\left(\frac{R}{\lambda_2}\right)\right)$ | $c_0^*\frac{R\lambda_1}{r^2}$, for $2R < r < \sqrt{R\lambda_1}$<br>$c_0^*\frac{\lambda_1}{r-R+\lambda}$, for $\lambda_2 < r-R < R$<br>$a^{-3}\left(\frac{af}{r-R+\lambda}\right)^{1/3}$, for $0 < r-R < \lambda_2$ |
| IIIa | $\sqrt{R\lambda_1}$ | $a^{-2}\sqrt{fN}\left(\sqrt{\frac{\lambda_1}{R}}-1+\ln\left(\frac{R}{\lambda_2}\right)\right)$ | $c_0^*\frac{R\lambda_1}{r^2}$, for $2R < r < \sqrt{R\lambda_1}$<br>$c_0^*\frac{\lambda_1}{r-R+\lambda}$, for $\lambda_2 < r-R < R$<br>$a^{-3}\left(\frac{af}{r-R+\lambda_3}\right)^{1/3}$, for $0 < r-R < \lambda_2$ |
| IV | $\sqrt{l_BQ\lambda_1}$ | $c_0^*\frac{(l_BQ\lambda_1)^{3/2}}{R^2}$ | $c_0^*\frac{l_BQ\lambda_1}{r^2}$, for $R < r < \sqrt{l_BQ\lambda_1}$ |
| V | $\sqrt{l_BQ\lambda_1}$ | $c_0^*\frac{(l_BQ\lambda_1)^{3/2}}{R^2}$ | $c_0^*\frac{l_BQ\lambda_1}{r^2}$, for $(R_0l_BQ\lambda_1)^{1/3} < r < \sqrt{l_BQ\lambda_1}$<br>$c_0^*\frac{(l_BQ\lambda_1)^{4/3}}{R_0^{1/3}r}$, for $R < r < (R_0l_BQ\lambda_1)^{1/3}$ |
| VI | $\sqrt{R\lambda_1}$ | $a^{-2}\sqrt{fN\frac{\lambda_1}{R}}$ | $c_0^*\frac{R\lambda_1}{r^2}$, for $(\lambda_2^2R)^{1/3} < r < \sqrt{R\lambda_1}$<br>$a^{-3}\frac{a^{1/3}f^{1/3}R^{2/3}}{r}$, for $2R < r < (\lambda_2^2R)^{1/3}$<br>$a^{-3}\left(\frac{af}{r-R+\lambda}\right)^{1/3}$, for $0 < r-R < R$ |

charge *Q*. Below we briefly summarize our results in various regimes of the adsorption diagram in Figure 6.

**Regime I (Stretched Planar Multilayers) ($\lambda_2 < \lambda < \lambda_1, \lambda_1 < R$).** In this regime polyampholyte chains are polarized and stretched by the external electric field of a particle. At distances $\lambda < r - R < \lambda_1$ the polymer density is hyperbolically decaying with distance $r - R$ (see Table 1). The adsorption stops at length scales on the order of $\lambda_1$ at which the polarization energy of a chain becomes on the order of the thermal energy $kT$. The polymer excess grows logarithmically with the surface charge density $\sigma$.

**Regime II (Planar Pseudo-Brush + Stretched Multilayers) ($\lambda_3 < \lambda < \lambda_2, \lambda_1 < R$).** Close to the surface at distances $r - R < \lambda$, the electric field created by the charged surface is almost constant. The sections of the

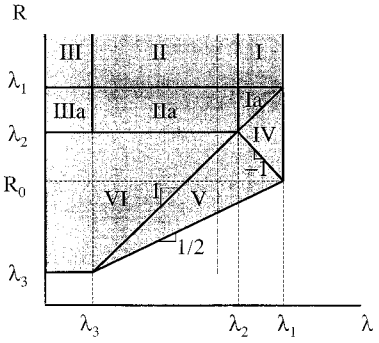


**Figure 6.** Adsorption diagram of polyampholyte chains as a function of the Gouy−Chapman length $\lambda$ and the particle size $R$. Adsorption region is shaded. Logarithmic scales.

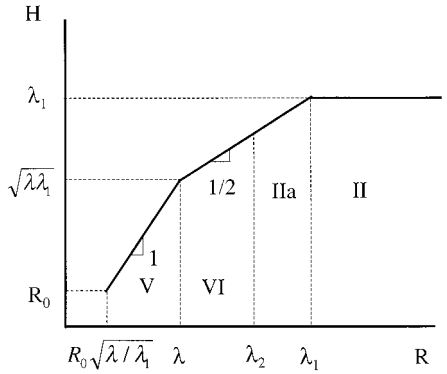


**Figure 7.** Dependence of the layer thickness H on the particle size $R$ at fixed surface charge density $\sigma \approx Q/R^2$ on the particle along the vertical dashed−dotted line in Figure 6. Logarithmic scales.

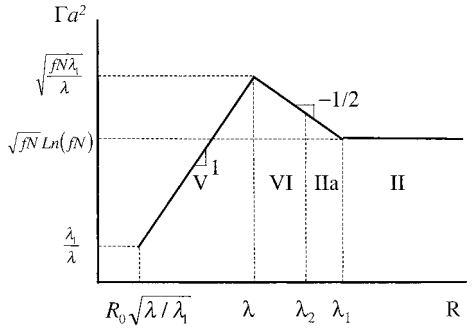


**Figure 8.** Nonmonotonic dependence of the surface coverage Γ on the particle size $R$ at fixed surface charge density $\sigma \approx Q/R^2$ on the particle along the vertical dashed−dotted line in Figure 6.

chains are uniformly stretched up to length scales on the order of the Gouy−Chapman length $\lambda$. On length scales $\lambda < r - R < \lambda_2$, the polyampholytes are stretched into a self-similar pseudobrush with polymer density decaying as $(r - R)^{-1/3}$. The size of the polymer chains in the first adsorbed layer is on the order of $\lambda_2$. At length scales larger than $\lambda_2$ adsorbed polyampholyte chains form stretched planar multilayers with polymer density inversely proportional to the distance from the charged surface.

**Regime III (Planar Saturated Pseudo-Brush + Stretched Multilayers) ($\lambda < \lambda_3$, $\lambda_1 < R$).** In this regime, the Gouy−Chapman length $\lambda$ is smaller than the root mean-square distance $af^{-1/2}$ between charged monomers along the chain. Near the charged surface inside a layer of thickness $\lambda_3$ the strands of polyampholytes are almost unperturbed by the external electric field and the monomer density is uniform. On length scales between $\lambda_3$ and $\lambda_2$, adsorbed polyampholytes form a self-similar pseudobrush similar to the one in regime II, and on length scales $\lambda_2 < r - R < \lambda_1$, the adsorbed chains form planar multilayers of stretched chains. In this regime the surface coverage reaches value $\Gamma \approx a^{-2}\sqrt{fN}\ln(fN)$ and becomes independent of the surface charge density.

The crossover into new regimes occurs when the particle size $R$ becomes on the order of the thickness $\lambda_1$ of the planar adsorbed layer. The line $R \approx \lambda_1$ defines the boundary between regimes I, II, III and Ia, IIa, IIIa in the adsorption diagram (Figure 6).

**Regimes Ia, IIa, IIIa (Spherical Multilayers + Adsorbed Layers of Regimes I, II, III)** In these regimes the curvature starts to affect the structure of the adsorbed layer at length scales $r > 2R$. At these length scales adsorbed polyampholytes are polarized in the hyperbolic electrostatic potential created by the charged sphere and form spherical multilayers of stretched chains. The polymer density in these layers is inversely proportional to the square of the distance to the particle surface and decays faster than that in the planar case (see Table 1). The adsorption stops at the distances on the order of $r_1 \approx \sqrt{R\lambda_1}$ where the polarization energy of a polyampholyte chain becomes on the order of the thermal energy $kT$. Close to the surface of the adsorbing particle, at length scales $0 < r - R < R$ the structure of the adsorbed layer is similar to the one in regimes I, II, and III, respectively.

**Regime IV (Weakly Charged Particles, Spherical Multilayers) ($\sqrt{fNR} < \lambda < \lambda_1$).** In this regime, the Gouy−Chapman length $\lambda$ is larger than the particle size $R$ and polyampholyte chains are polarized and stretched by the unscreened electrostatic potential of the charged sphere carrying charge $eQ$. The adsorbed polyampholyte chains form spherical multilayers of stretched chains in which the polymer density decays as $c \sim r^{-2}$. The thickness of the adsorbed layer $r_1 \approx \sqrt{l_B Q\lambda_1}$ increases with increasing charge $Q$ of the particle.

**Regime V (Weakly Charged Particles, Pseudo-Star + Spherical Multilayers) ($R < \lambda < \sqrt{fR^2}$, $\lambda < \sqrt{fNR_0^2/R}$).** Close to the particle surface, polyampholyte chains form a self-similar structure similar to that of a neutral starlike macromolecule, with the number of arms $n_{ch} \simeq f^{2/3}(l_B Q/a)^{4/3}$ and with the degree of polymerization $N$ each. This adsorbed state of polyampholytes is called a "pseudo-star". The thickness of this first layer is equal to $r_2 \approx (a^2 l_B Q f^{1/2} N^{3/2})^{1/3}$. On length scales $r_2 < r < r_1$ the adsorbed chains form spherical multilayer of stretched chains with the polymer density decaying as $r^{-2}$.

**Regime VI (Strongly Charged Particles, Pseudo-Star + Spherical Multilayers) ($af^{-1/2} < R < \lambda_2$, $\lambda < R$).** In this regime at length scales between $2R$ and $r_2$, the adsorbed chains form a pseudo-star. Close to the particle surface for $0 < r - R < R$, the curvature of the adsorbing particle does not affect the structure of the adsorbed layer and polyampholytes form a planar pseudo-brush. The polymer density profile and surface coverage in this regime are given in Table 1.

Figures 7 and 8 show the dependence of the thickness of the adsorbed layer $H$ and surface coverage Γ on a particle size $R$ for a fixed value of the surface charge density $\sigma \approx Q/R^2$ along the vertical dashed−dotted line in Figure 6. For a particle larger than the marginal

Gouy−Chapman length $\lambda_1 \approx \sqrt{fN}R_0$ (regime II of the diagram in Figure 6), the adsorbed polyampholyte chains do not "feel" the curvature of the particle, and the layer thickness $H$ and surface coverage $\Gamma$ are independent of the particle size $R$ ($H \approx \lambda_1 \approx \sqrt{fN}R_0$, $\Gamma \approx a^{-2}\sqrt{fN}$ ln $fN$). The outer layers of adsorbed chains are affected by the particle curvature as soon as the size of the particle $R$ becomes comparable with the layer thickness $\lambda_1$.

For smaller particles ($R < \lambda_1$) the polarization of polyampholyte chains in the outer layers at the length scales $r > R$ occurs in the screened electric field created by the charged particle with the effective charge $Q_{\text{eff}} \approx R/l_B$ (see section IIIA for details). In this case the deformation of a polyampholyte chain from its Gaussian conformation begins at distance $r_1 \approx \sqrt{\lambda_1 R}$, that is the thickness $H$ of the adsorbed layer. In this regime the layer thickness $H$ decreases while the surface coverage $\Gamma$ increases as square root of the particle size $R$. These power law dependences continue as long as the particle size $R$ is larger than the Gouy−Chapman length $\lambda$.

If the particle size decreases further $R < \lambda$ the adsorbed polyampholyte chains are polarized by the unscreened electric field of the charged sphere with charge $Q$ (see section IIIB regime V of the diagram in Figure 6). The deformation of polyampholyte chains from their Gaussian conformations begins at the distance $r \approx H \approx R\sqrt{\lambda_1/\lambda}$. In this regime the thickness of the adsorbed layer $H$ and the surface coverage $\Gamma$ changes linearly with the particle size $R$. Finally, chains desorb from the particle when the thickness of the adsorbed layer $H$ becomes on the order of the Gaussian size of the polyampholyte chain $R_0$. This happens at particle size $R$ on the order of $R_0\sqrt{\lambda/\lambda_1}$.

For example, for a chain with $N = 500$ monomers, with the fraction of charges $f = 0.02$, and with the bond length $a = 3$ Å in the solution with Bjerrum length $l_B = 7$ Å, the adsorption threshold on the charged surface is at $\sigma_1 \approx 7 \times 10^{-4}$ Å$^{-2}$ and the marginal Gouy−Chapman length $\lambda_1 \approx 200$ Å. The crossover to self-similar adsorbed layer occurs at $\lambda_2 \approx 120$ Å ($\sigma_2 \approx 10^{-3}$ Å$^{-2}$). The thickness of the polymeric adsorbed layer around strongly charged spherical particle with size $R \approx 150$ Å is $r_1 \approx \sqrt{R\lambda_1} \approx 173$ Å.

The theory, presented above, is only valid for soluble polyampholytes. In order for a polyampholyte chain to be soluble, the fluctuation-induced attractive interaction between charged monomers should be weaker than the thermal energy $kT$. This attraction is on the order of the thermal energy $kT$ per Debye volume $r_D^3$, where $r_D \approx (l_B Nf/R^3)^{-1/2}$. If there are many Debye volumes per chain ($r_D \ll R$), this attraction is strong, and the polyampholyte with equal numbers of $Nf_+$ positively charged and of $Nf_-$ negatively charged monomers forms a compact globule[40−43] and precipitates from solution. But if the Debye radius is larger than the chain size ($r_D > R$) the attraction is weak and the chain remains almost unperturbed. The condition $r_D > R_0$ for a Gaussian chain of radius $aN^{1/2}$ can be written in terms of the fraction of charged groups $f < (u\sqrt{N})^{-1}$ where $u = l_B/a$ is the ratio of the Bjerrum length $l_B$ to the bond size $a$.

Another effect that was neglected in the paper is renormalization of the external electric field by the polarized chains. We have ignored the electrostatic interactions between chains. These interactions become important when the polarization energy density of the chains in the adsorbed layer approaches the energy density of the electric field created by the charged object. For adsorption on the planar surface these interactions are unimportant as long as the fraction of the charged monomers $f$ on a chain is smaller than $u^{-4/5}N^{-3/5}$.[22] Similar estimate is valid for adsorption on a spherical particle.[44] For example, for polyampholyte adsorption in regime V of the adsorption diagram in Figure 6, the polarization energy density at the length scales $R < r < r_2$ is

$$|U_{\text{pol}}(r)| \approx kTa^6c(r)^3 \approx kT\frac{f(l_BQ)^2}{a^2r^3} \tag{56}$$

(see section IIIB for details). This polarization energy $U_{\text{pol}}(r)$ is smaller than the self-energy density of the electric field created by a charged particle

$$U_{s-e}(r) \approx kT\frac{l_BQ^2}{r^4}$$

as long as

$$r < r^* \approx \frac{a^2}{l_Bf} \tag{57}$$

To ignore the interactions between polyampholyte chains on all length scales $R < r < r_2$, $r^*$ has to be larger than $r_2$. This condition can be rewritten in terms of the particle size $R$ and the Gouy−Chapman length $\lambda$ as follows

$$R < \sqrt{\lambda}\frac{a^2}{l_B^{3/2}f^{7/4}N^{3/4}} \tag{58}$$

The regime V of the adsorption diagram in Figure 6 is inside this region ($\lambda_2^{1/2} < a^2l_B^{-3/2}f^{-7/4}N^{-3/4}$) if the fraction of the charged monomers $f$ on the chain is smaller than $u^{-4/5}N^{-3/5}$. Thus, for weakly charged polyampholytes $f < u^{-4/5}N^{-3/5}$ the renormalization of the local electric field by adsorbed polyampholyte chains can be neglected in all regimes of the diagram in Figure 6.

Finally, let us comment on the effect of added salt. The presence of the salt results in the exponential screening of the electrostatic potential at distances larger than the Debye screening length $r_D$. The thickness and structure of the adsorbed layer does not change as long as the Debye screening length is larger than the marginal Gouy−Chapman length $\lambda_1$ for charged surface and $r_1$ for spherical particle. For the above example of a polyampholyte chain, the Debye screening length $r_D$ should be larger than 200 Å and corresponding concentration of salt should be smaller than $c_{\text{salt}} \approx 2 \times 10^{-4}$ M. We will consider the effects of added salt in a separate publication.

**Acknowledgment.** The financial support of the NSF under Grant DMR-9730777 and of the Eastman Kodak Co. is gratefully acknowledged. Authors are grateful to Dr. T. Whitesides for valuable discussions.

## Appendix

**Planar Symmetry.** To describe the polydisperse brush of loops near the charged planar surface we will use the strong stretching approximation and assume

that all loops with a given charge distribution $\{q(t)\}$ are stretched in the same way. This means that all middle points of the loops containing $2g$ monomers are located at the same distance $z(g)$ from the surface−Alexander−deGennes approximation[45,46] for the polydisperse brush.[47] The total free energy of the loop includes three terms

$$F_g = F^g_{elast} + W^g_{pol} + W^g_{rep} \quad (59)$$

The elastic energy $F^g_{elast}$ of the loop is

$$\frac{F^g_{elast}}{kT} \approx \frac{1}{2a^2}\int_0^g \left(\frac{dz_g(t)}{dt}\right)^2 dt \quad (60)$$

The electrostatic energy of the loop with $2g$ monomers with a charge distribution $\{q(t)\}$ in the logarithmic electrostatic potential $-kT\ln(1 + z(t)/\lambda)$ is

$$W^g_{pol}(\{q(t)\}) \approx -2kT\int_0^g q(t)\ln\left(1 + \frac{z_g(t)}{\lambda}\right) dt \quad (61)$$

The monomers in the loops also interact with each other through the short-range excluded volume interactions. In the mean-field approximation this interaction can be replaced by the effective external potential $h(z)$. The dependence of the external potential $h(z)$ on the coordinate $z$ has to be found self-consistently. The contribution $W^g_{rep}$ from the short-range interactions to the loop free energy is

$$W^g_{rep} \approx kT\int_0^g h(z_g(t))\, dt \quad (62)$$

Combining elastic, electrostatic, and excluded volume contributions, one obtains the total free energy of the loop containing $2g$ monomers with a given charge distribution $q(t)$

$$\frac{F_g}{kT} \approx \frac{1}{2a^2}\int_0^g \left(\frac{dz_g(t)}{dt}\right)^2 dt - 2\int_0^g q(t)\ln\left(1 + \frac{z_g(t)}{\lambda}\right) dt + \int_0^g h(z_g(t))\, dt \quad (63)$$

In the strong stretching approximation the trajectory of a polymer chain is determined by the classical path of the functional (63)

$$a^{-2}\frac{d^2 z_g(t)}{dt^2} = -\frac{2q(t)}{\lambda + z_g(t)} + \frac{dh(z_g(t))}{dz_g(t)} \quad (64)$$

with the boundary conditions $z_g(0) = 0$ and $dz_g(g)/dt = 0$ which corresponds to the zero tension at the middle of the loop. Multiplying both parts of the extremal eq 64 by $dz_g(t)/dt$, we obtain the "conservation law" for the "particle" traveling along the trajectory $z_g(t)$ in the external potential

$$\frac{d}{dt}\left(\frac{1}{2a^2}v_g^2(t) - h(z_g(t))\right) = -\frac{2q(t)}{\lambda + z_g(t)}v_g(t) \quad (65)$$

where $v_g(t) = dz_g(t)/dt$ is the local stretching of the loop given by the following integral equation

$$a^{-2}v_g(s) = 2\int_s^g \frac{q(t)}{\lambda + z_g(t)}dt - \int_s^g \frac{dh(z_g(t))}{dz}dt \quad (66)$$

To proceed further, we will assume a random distribution of charged monomers in the loop with average value $\langle q(t)\rangle = 0$ and the delta-functional correlations $\langle q(t)q(t')\rangle = f\delta(t - t')$. Averaging both sides of eqs 64 and 65 with respect to the charge distributions in the loop and keeping only the first nonzero terms, we obtain equations describing the average stretching

$$a^{-2}\frac{d\langle v_g(t)\rangle}{dt} = \frac{dh(\langle z_g(t)\rangle)}{dz} \quad (67)$$

and the mean-square stretching

$$\frac{d}{dt}\left(\frac{1}{2a^2}\langle v_g^2(t)\rangle - h(\langle z_g(t)\rangle)\right) = -\frac{2a^2 f}{(\lambda + \langle z_g(t)\rangle)^2}, \quad \text{for } t < g \quad (68)$$

of a loop with a typical charge distribution. In derivation of the last two equations we have assumed that $\langle q(s)h(\langle z_g(t)\rangle)\rangle$ is equal to 0 and charge-local deformation correlation function $\langle q(t)v_g(t)\rangle$ is equal to $a^2 f/(\lambda + \langle z_g(t)\rangle)$ for $t < g$ and zero otherwise.

In the strong stretching approximation, we can transform the derivative $d/dt$ into the derivative $d/dz$. For example, for the average local stretching $\langle v_g(t)\rangle$ we can write

$$\frac{d\langle v_g(t)\rangle}{dt} = \frac{dz_g(t)}{dt}\frac{d\langle v_g(t)\rangle}{dz} \approx \frac{d}{dz}\frac{\langle v_g(t)\rangle^2}{2} = a^2\frac{dh(z)}{dz} \quad (69)$$

Using this identity we can solve the differential equation eq 67 for the function $\langle v_g(t)\rangle$ in terms of the effective external potential $h(z)$.

$$\frac{\langle v_g(z)\rangle^2}{2a^2} = h(z) - h(z_g) \quad (70)$$

where $z_g$ is the middle point of the loop. The last equation can also be rewritten in the integral form that gives the relation between the number of monomers in a loop and its middle point position $z_g$

$$g = \frac{1}{a\sqrt{2}}\int_0^{z_g}\frac{dz}{\sqrt{h(z) - h(z_g)}} \quad (71)$$

Substituting the expression for the local stretching (eq 66) into the expression for the free energy (eq 63) and averaging it over all possible distribution of charged monomers along the chain $\{q(t)\}$, we obtain the average free energy of the loop with $2g$ monomers as a functional of the effective external potential $h(z)$.

$$\frac{\langle F_g(\{h(z)\})\rangle}{kT} \approx -gh(z_g) + 2\int_0^g h(z_g(t))\, dt + 2a^2 f\int_0^g ds\int_s^g \frac{dt}{(\lambda + \langle z_g(t)\rangle)^2} - 4a^2 f\int_0^g \frac{dt}{\lambda + \langle z_g(t)\rangle}\int_0^t \frac{ds}{\lambda + \langle z_g(s)\rangle} \quad (72)$$

In the derivation of the last equation, we have used the identity

$$\langle\int_0^g ds\, q(s)\ln(\lambda + z_g(s))\rangle = \left\langle\int_0^g ds\, q(s)\int_0^s \frac{v_g(t)dt}{\lambda + z_g(t)}\right\rangle \quad (73)$$

To find the total free energy of the adsorbed layer of thickness $\lambda_2$ we have to sum the contribution from all loops in the layer. For the adsorbed layer with loop distribution function $\rho_g$—the number of loops with $2g$ monomers per unit area—the free energy is

$$F_{\lambda_2} \approx kTA \int_{g_{cut}}^{N} \rho_g \left( \frac{\langle F_g(\{h(z)\}) \rangle}{kT} + \ln\left(\frac{\rho_g}{e}\right) \right) dg - \int_0^{\lambda_2} \left( h(z) - \frac{a^6 c(z)^2}{3} \right) c(z)\, dz \quad (74)$$

where $A$ is the area of the adsorbing surface. The minimum of the functional (74) is searched with respect to the effective external potential $h(z)$, the local monomer concentration $c(z)$, and the loop distribution function $\rho_g$ with the additional constraint

$$\int_{g_{cut}}^{N} \rho_g g\, dg = \int_0^{\lambda_2} c(z)\, dz \quad (75)$$

that determines the correct normalization of the loop distribution function $\rho_g$. The integration in the functional eq 74 starts from the loops of size $g_{cut} \approx f^{-1}$ that have at least one charged monomer in them. Minimization of the functional (74) with respect to monomer concentration $c(z)$ and loop distribution function $\rho_g$ results in the following system of equations

$$h(z) = a^6 c(z)^2 + \mu \quad (76)$$

$$\ln \rho_g = \mu g - \frac{\langle F_g(\{h(z)\}) \rangle}{kT} \quad (77)$$

where $\mu$ is the Lagrange multiplier corresponding to the constraint eq 75. In general case in order to find the form of the effective external field we have to take variational derivative of the functional eq 74 with respect to $h(z)$ and solve the full system of integral and ordinary equations. In our case we can make a shortcut and guess the form of the function $h(z)$ from the analysis of eqs 67 and 68. From these equations, we can conclude that $(\langle v_g(z) \rangle^2)_z = a^2 h(z)_z$ and $\langle v_g(z) \rangle (\langle v_g^2(z) \rangle)_z \approx a^2 \langle v_g(z) \rangle h(z)_z \approx a^4 f (z + \lambda)^{-2}$ which allows us to choose

$$h(z) \approx C \left( \frac{af}{z + \lambda} \right)^{2/3} \quad (78)$$

where $C$ is a numerical constant. The exact value of the numerical constant $C$ can be found by using $h(z)$ as a trial function with an adjustable parameter $C$. The further simplification follows from the fact that the Lagrange multiplier $\mu$ is small. It is on the order of $h(\lambda_2)$, and in the first approximation, we can set the local monomer density

$$c(z) \approx a^{-3} \sqrt{h(z)} = a^{-3} \sqrt{C} \left( \frac{af}{z + \lambda} \right)^{1/3} \quad (79)$$

Taking this fact into account, we can write the integral relation for the loop distribution function

$$\int_{g_{cut}}^{N} \rho_g g\, dg = \int_0^{\lambda_2} c(z)\, dz \approx f^{1/3} \sqrt{C} (\lambda_2^{2/3} - \lambda^{2/3}) \quad (80)$$

The rhs of the last equation is dominated by the upper limit of the integral and is proportional to $N^{1/2}$ ($\lambda_2 \sim f^{1/4} N^{3/4}$). To obtain the same power law dependence on the degree of polymerization $N$ from the integration of the loop distribution function $\rho_g$, this function has to be a power law function $f^{1/2} g^{-3/2}$. To match the value of the integral in the rhs of eq 80 at the lower limit $z = 0$ with the value of the integral in the lhs, the loop distribution function has to be equal to 0 for the loops with sizes smaller than $g_\lambda \approx f^{-1/3} \lambda^{4/3}$. Let us verify that the value $g_\lambda$ can be obtained from the scaling relation between the average loop size and the number of monomers in it

$$g \approx \frac{1}{a} \int_0^{z_g} \frac{dz}{\sqrt{h(z) - h(z_g)}} \approx f^{-1/3} C^{-1/2} a^{-4/3} l^{1/3} \sqrt{l^{2/3} - \lambda^{2/3}} (\lambda^{2/3} + 2l^{2/3}) \quad (81)$$

where we defined $l = z_g + \lambda$. For the loops with the size $z_g$ on the order of the Gouy−Chapman length $\lambda$ the number of monomers in them is on the order of $f^{-1/3} \lambda^{4/3}$. Thus, the integral in eq 80 is solved by the loop distribution function of the form

$$\rho_g \approx \begin{cases} a^{-2} f^{1/2} g^{-3/2}, & \text{for } g_\lambda < g < N \\ 0, & \text{for } g < g_\lambda \end{cases} \quad (82)$$

Let us now verify that the Lagrange multiplier $\mu$ is indeed on the order of $h(\lambda_2)$. To prove it we have to rewrite eq 77 in the following form

$$\mu = \frac{\int_{g_{cut}}^{N} \rho_g (\ln \rho_g + \langle F_g(\{h(z)\}) \rangle / kT)\, dg}{\int_0^{\lambda_2} c(z)\, dz} \approx \frac{f^{2/3}}{\lambda_2^{2/3}} \ln N \quad (83)$$

where we use the fact that the free energy of the loop $\langle F_g(\{h(z)\}) \rangle \approx kT\sqrt{fg}$ is on the order of the thermal energy $kT$ times the typical charge fluctuations $\sqrt{fg}$ in the halves of the loop.

**Spherical Symmetry.** The description of the curved self-similar polymer layer is similar to the one presented above for the planar case with one modification. This modification is related to the loop electrostatic energy.

$$W_{pol}^{g}(\{q(t)\}) \approx kT \int_0^{g2R} q(t) \left( \frac{l_B Q}{R} - \ln\left(1 + \frac{r - R}{\lambda}\right) \right) dt + \int_{g2R}^{g} q(t) \left( \frac{l_B Q_{eff}}{r} + \frac{l_B Q}{R} - \ln\left(1 + \frac{R}{\lambda}\right) \right) dt \quad (84)$$

This expression reduces to the planar case for the loops with size $r_g$ smaller than the radius $R$ of the particle. The distribution function $\rho_g$ of such loops and polymer concentration $c(r)$ are given by eqs 82 and 79, respectively. For the loops with size $r_g$ larger than the particle size $R$ or with the number of monomers $g \gg g_{2R}$ we can neglect the first term in the rhs of eq 84 and consider the stretching of the loop in the hyperbolic electrostatic potential of a charged sphere with effective charge $Q_{eff}$. Below we will consider only the second case of loops, $g \gg g_{2R}$.

Combining once again elastic, electrostatic, and excluded volume contributions to the total free energy, one obtains the total free energy of the loop containing $2g$ monomers with a given charge distribution $q(t)$ in the following form

$$\frac{F_g}{kT} \approx \frac{1}{2a^2}\int_0^g \left(\frac{dr_g(t)}{dt}\right)^2 dt + \int_0^g q(t)\frac{l_B Q_{eff}}{r_g(t)}\,dt + \int_0^g h(r_g(t))\,dt \quad (85)$$

In the strong stretching approximation the trajectory of the polymer chain is determined by the classical path of the functional (85)

$$a^{-2}\frac{d^2 r_g(t)}{dt^2} = -q(t)\frac{l_B Q_{eff}}{r_g^2(t)} + \frac{dh(r_g(t))}{dr} \quad (86)$$

The energy conservation in the stretched loop leads to

$$\frac{d}{dt}\left(\frac{1}{2a^2}v_g^2(t) - h(r_g(t))\right) = -q(t)\frac{l_B Q_{eff}}{r_g^2(t)}v_g(t) \quad (87)$$

where $v_g(t) = dr_g(t)/dt$ is the local stretching of the loop given by the following integral equation:

$$a^{-2}v_g(s) = \int_s^g q(t)\frac{l_B Q_{eff}}{r_g^2(t)}dt - \int_s^g \frac{dh(r_g(t))}{dr}dt \quad (88)$$

For the random charge distribution with zero average value $\langle q(t)\rangle = 0$ and $\delta$-functional correlations $\langle q(t)q(t')\rangle = f\delta(t - t')$, one can obtain for the average stretching

$$a^{-2}\frac{d\langle v_g(t)\rangle}{dt} = \frac{dh(\langle r_g(t)\rangle)}{dr} \quad (89)$$

and for the mean-square stretching

$$\frac{d}{dt}\left(\frac{1}{2a^2}\langle v_g^2(t)\rangle - h(\langle r_g(t)\rangle)\right) = -\frac{a^2 f (l_B Q_{eff})^2}{2\langle r_g(t)\rangle^4}, \quad \text{for } t < g \quad (90)$$

of a loop with a typical charge distribution.

We again transform the derivative d/d$t$ into the derivative d/d$r$. After this transformation, the differential equation for the average local stretching $\langle v_g(t)\rangle$ is

$$\frac{d\langle v_g(t)\rangle}{dt} = \frac{dr_g(t)}{dt}\frac{d\langle v_g(t)\rangle}{dr} \approx \frac{d}{dr}\frac{\langle v_g(t)\rangle^2}{2} = a^2\frac{dh(r)}{dr} \quad (91)$$

The form of the function $h(r)$ can now be determined from the analysis of the equations (90, 91). It follows from these equations that $(\langle v_g(r)\rangle^2)_r = a^2 h(r)_r$ and $\langle v_g(r)\rangle(\langle v_g^2(r)\rangle)_r \approx a^2\langle v_g(r)\rangle h(r)_r \approx a^4 f (l_B Q_{eff})^2 r^{-4}$ which allows us to choose the effective external potential $h(r)$ in the following form

$$h(r) \approx C\frac{f^{2/3}a^{2/3}l_B^{4/3}Q_{eff}^{4/3}}{r^2} \quad (92)$$

where $C$ is a numerical constant. In this effective external potential $h(r)$ the dependence of number of monomers in the loop on its middle point position $r_g$ is

$$g = \frac{1}{a\sqrt{2}}\int_{2R}^{r_g}\frac{dr}{\sqrt{h(r) - h(r_g)}} \approx r_g^2 a^{-4/3}l_B^{-2/3}f^{-1/3}Q_{eff}^{-2/3} \quad (93)$$

The self-similar brush of loops ends at the distance $r_2 \approx a^{2/3}(l_B f^{1/2}Q_{eff})^{1/3}N^{1/2}$ when the number of monomers in the loop becomes on the order of the degree of polymerization $N$ of polyampholyte chains.

The effective potential $h(r)$ for a $\Theta$ solvent is proportional to the probability of the three body contacts $a^6 c(r)^2$. The monomer density distribution in the adsorbed layer can be written as

$$c(r)a^3 \approx \frac{f^{1/3}a^{1/3}l_B^{2/3}Q_{eff}^{2/3}}{r} \quad (94)$$

The loop distribution function $\rho_g$ in the layer of the thickness $r_2$ can be found from the following integral equation:

$$\int_{g_{2R}}^N \rho_g g\,dg = \frac{1}{R^2}\int_{2R}^{r_2} c(r)r^2 dr \approx \frac{N}{R^2}\left(\frac{l_B^2 Q_{eff}^2 f}{a^2}\right)^{2/3} \quad (95)$$

The solution of this equation is a $\delta$ function

$$\rho_g \approx \frac{1}{R^2}\left(\frac{l_B^2 Q_{eff}^2 f}{a^2}\right)^{2/3}\delta(g - N), \quad \text{for } g_{2R} < g < N \quad (96)$$

## References and Notes


(1) Kawaguchi, M.; Takahashi, A. *Adv. Colloid Interface Sci.* **1992**, *37*, 219.
(2) Fleer, G. J.; Cohen Stuart, M. A.; Scheutjens, J. M. H. M.; Gasgove, T.; Vincent, B. *Polymer at Interfaces*; Chapman and Hall: London, 1993.
(3) Bajpai, A. K. *Prog. Polym. Sci.* **1997**, *22*, 523.
(4) de Gennes, G.-P. *Macromolecules* **1981**, *14*, 1637.
(5) Wang, T. K.; Audebert, R. *J. Colloid. Interface Sci.* **1988**, *121*, 32.
(6) Shubin, V.; Linse, P. *J. Phys. Chem.* **1995**, *99*, 1285.
(7) Wiegel, F. W. *J. Phys. A* **1977**, *10*, 299.
(8) Wiegel, F. W. In *Phase Transition and Critical Phenomena*; Domb, C., Leibowitz, J. L., Eds.; Academic Press: New York, 1983; v.7.
(9) Odijk, T. *Macromolecules* **1980**, *13*, 1542.
(10) Muthukumar, M. *J. Chem. Phys.* **1987**, *86*, 7230.
(11) Borisov, O. V.; Zhulina, E. B.; Birshtein, T. M. *J. Phys. II (Fr.)* **1994**, *4*, 913.
(12) Van der Schee, H. A.; Lyklema, J. *J. Phys. Chem.* **1984**, *88*, 6661.
(13) Blaakmeer, J.; Bohmer M. R.; Cohen Stuart, M. A.; Fleer, G. J. *Macromolecules* **1990**, *23*, 2301.
(14) Bohmer M. R.; Evers O. A.; Scheutejens, J. M. H. M. *Macromolecules* **1990**, *23*, 2288.
(15) Varoqui, R.; Johner, A.; Elaissari, A. *J. Chem. Phys.* **1991**, *94*, 6873.
(16) Borukhov, I.; Andelman, D.; Orland, H. *Europhys. Lett.* **1995**, *32*, 499.
(17) Chatellier, X.; Joanny, J.-F. *J. Phys. II* **1996**, *6*, 1669.
(18) Borukhov, I.; Andelman, D.; Orland, H. *Macromolecules* **1998**, *31*, 1665.
(19) Kong, C. Y.; Muthukumar, M. *J. Chem. Phys.* **1998**, *109*, 1522.
(20) Dobrynin, A. V.; Rubinstein, M.; Joanny, J.-F. *Macromolecules* **1997**, *30*, 4332.
(21) Netz, R.; Joanny, J.-F. *Macromolecules* **1998**, *31*, 5123.
(22) Dobrynin, A. V.; Obukhov, S. P.; Rubinstein, M. *Macromolecules* **1999**, *32*, 5689.
(23) Curme, H. G.; Natale, C. C. *J. Phys. Chem.* **1964**, *68*, 3009.
(24) Berendsen, R.; Borginon, H. *J. Photogr. Sci.* **1968**, *16*, 194.
(25) Maternaghan, T.; Banghan, O. B.; Ottewill, R. H. *J. Photogr. Sci.* **1980**, *28*, 1.
(26) Kudish, A. T.; Eirich, F. R. *Proteins at Interfaces*; American Chemical Society: Washington, DC, 1987, Vol. 261.
(27) Kawanishi, N.; Christenson, H.; Ninham, B. *J. Phys. Chem.* **1990**, *94*, 4611.
(28) Vaynberg, A. K.; Wagner, N. J.; Sharma, R.; Martic, P. *J. Colloid Interface Sci.* **1998**, *205*, 131.
(29) Kamiyama, Y.; Israelachvili, J. *Macromolecules* **1992**, *25*, 5081.
(30) Neyret, S.; Ouali, L.; Candau, F.; Pefferkorn, E. *J. Colloid Interface Sci.* **1995**, *187*, 86.
(31) Schiessel, H.; Blumen, A. *J. Chem. Phys.* **1996**, *105*, 4250.

(32) Schiessel, H.; Oshanin, G.; Blumen, A. *J. Chem. Phys.* **1995**, *103*, 5070.
(33) Schiessel, H.; Oshanin, G.; Blumen, A. *Macromol. Theor. Simul.* **1996**, *5*, 45.
(34) Schiessel, H.; Blumen, A. *J. Chem. Phys.* **1996**, *104*, 6036.
(35) Schiessel, H.; Blumen, A. *Macromol. Theor. Simul.* **1997**, *6*, 103.
(36) Israelachvilli, J. N. *Intermolecular and Surface Forces*; Cornell University Press: Ithaca, NY, 1985.
(37) Alexander, S.; Chaikin, P. M.; Grant, P.; Morales, G. J.; Pincus, P. *J. Chem. Phys.* **1984**, *80*, 5776. According to this paper at high values of the bare charge $Q$ the effective charge $Q_{eff}$ demonstrates weak (logarithmic) dependence on $Q$. In our scaling consideration we ignore all logarithmic corrections and consider $Q_{eff}$ to be constant above the threshold value $R/l_B$.
(38) Daoud, M.; Cotton, J.-P *J. Phys. (Paris)* **1982**, *43*, 531.
(39) Birshtein, T. M.; Zhulina, E. B. *Polymer* **1984**, *25*, 1453.
(40) Higgs, P. G.; Joanny, J. F. *J. Chem. Phys.* **1988**, *89*, 5273.
(41) Kantor, Y.; Kardar, M.; Li, H. *Phys. Rev. Lett.* **1992**, *69*, 61; *Phys. Rev. E* **1994**, *49*, 1383.
(42) Kantor, Y.; Kardar, M. *Europhys. Lett.* **1994**, *27*, 643; *Phys Rev. E* **1995**, *51*, 1299; **1995**, *52*, 835.
(43) Dobrynin, A. V.; Rubinstein, M. *J. Phys. II (Fr.)* **1995**, *5*, 677.
(44) Zhulina, E. B.; Dobrynin, A. V.; Rubinstein, M. *Eur. Phys. J. E*, in press.
(45) Alexander, S. I. *J. Phys. (Paris)* **1977**, *38*, 977.
(46) de Gennes, P.-G. *Macromolecules* **1980**, *13*, 1069.
(47) Aubouy, M.; Guisselin, O.; Raphael, E. *Macromolecules* **1996**, *29*, 7261.

MA000706D